A RAPID SCHEME FOR ESTIMATING TRANSITION ON WINGS BY LINEAR STABILITY THEORY

M GASTER & F JIANG
Cambridge University Engineering Department

Renewed interest in laminar flow aircraft has created the need for faster methods of predicting transition than are at present available. The most commonly used technique, the e^N method, is based on linear stability theory. Transition is generally found to occur roughly where the amplification of linear waves exceeds some empirical threshold. The calculations needed to predict this location require the evaluation of a large number of eigenvalues of the Orr-Sommerfeld equation. This is both time consuming and expensive. The scheme has its merits, but is too unwieldy for routine design purposes.

It is shown here that the calculations of wave growth can be carried out very much faster by introducing further approximations. In this discussion only two-dimensional incompressible flows are considered as the first stage of the development of a fully three-dimensional design tool.

The velocity profiles on a wing designed for extensive regions of laminar flow have relatively weak pressure gradients in the critical regions of the boundary layer and can be modeled well by the Falkner-Skan family. The dispersion relationship linking wave growth to frequency and Reynolds number were represented by a set of two-variable Padé approximants for a range of Falkner-Skan profiles. The wing boundary layer velocity profiles were matched locally to the similarity pressure gradient parameter so that appropriate Padé coefficients could be found from the precomputed tables. The calculation of the amplification curves could then be carried out very quickly indeed. Not only was the calculation performed some 500-1000 faster than by the direct Orr-Sommerfeld approach, but the differences in estimating 'N' turned out to be less than 3%. In view of approximations already used in the Orr-Sommerfeld approach this difference is of no consequence.

The extension to a fully three-dimensional scheme appears to be straightforward.

1. Introduction

The next generation of large transport aircraft could well benefit from laminar flow, and the estimation of the transition to turbulent flow is a necessary requirement for design. The most commonly used prediction scheme based on linear theory is the well-known e^N method. The boundary layer on the wing is assumed to be known and the spatial amplification rate of eigenmodes of different frequencies are computed so that the 'N' factor can be found (Mack 1977). The task is time-consuming and tedious if the required eigenvalues are calculated by solving the Orr-Sommerfeld equation directly. The requirement of relatively large amounts of computing time prevents stability studies from being used for a wide range of different wing designs and flight conditions. In this paper, we present a method for the rapid estimation of eigenvalues that can be used to calculate wave growth in the boundary layers of wings. For the incompressible case, we assume that the non-similar laminar boundary layer on the aircraft wing can be represented accurately enough by the one parameter similarity family of Falkner-Skan, the pressure gradient parameter defining the profile as a function of the streamwise location. The value of this parameter was determined by matching the displacement thickness and either the second derivative of the profile at the wall, or the momentum thickness of the boundary-layer with the Falkner-Skan family. Then the eigenvalue relation of the boundary layer profiles can be estimated from those of the Falkner-Skan family which will be represented by some simple analytic expressions.

The feasibility of approximating the eigenvalue relation by simple elementary analytic expressions is based on the fact that the Orr-Sommerfeld equation defines an analytic dispersion relation $\Delta(\alpha, \omega, R) = 0$, except at isolated branch points. This was first sug-

gested by Gaster (1968), and later effected by Gaster & Jordinson (1975), who used a power series representation to approximate the eigenvalues in some region of the wavenumber-frequency plane in their studies of the Blasius boundary layer flow. Gaster (1978) further demonstrated that the rate of convergence of this series could be vastly improved by resorting to the Shanks nonlinear transformation (Shanks 1955). This idea of exploring the analytic properties of the eigenvalues was followed by Jiang (1990) who extended the power series technique through the use of the Padé approximant (Baker & Graves-Morris 1981) to construct an analytic rational-fraction function for the eigenvalue relation. This approach was suggested by Gaster (1978) as an alternative scheme to improve the convergence of the power series representation. The Padé approximant method has certain advantages over the power series representation in that its validity is not limited to a convergence circle. It gives better accuracy over a wider region by representing a function by a ratio of two polynomials, essentially mapping singularities to infinity. Its advantages over the Shanks transformation come from its explicit expression whose analyticity can be analysed, whereas, the Shanks transformation only offers a blind iterative process. Although the Shanks transformation can extend the usable region of the power series, its accuracy is limited by the fact that it introduces artificial singularities. On the other hand, it is always possible to choose one of the Padé approximants which is free from these artificial singularities in the region of interest.

2. Eigenvalue problem

Consider a two-dimensional incompressible boundary layer aligned along the $\hat{x}$-axis of a Cartesian coordinate system $(\hat{x}, \hat{y})$ perturbed by a small external disturbance. Here $(\hat{x}, \hat{y})$ is used to denote dimensional coordinates and a caret $\hat{}$ will be used to denote dimensional physical quantities. The disturbance is assumed to be of small amplitude so that the use of linear theory is justified. In this case, the disturbance velocity v in the y direction is governed by the fourth-order Orr-Sommerfeld equation, in a non-dimensional form,

$$v'''' - 2\alpha^2 v'' + \alpha^4 v - i\alpha R(\overline{U} - \omega/\alpha)(v'' - \alpha^2 v) + i\alpha R\overline{U}'' v = 0, \qquad (2.1)$$

where α, ω and R are respectively the wavenumber, frequency and Reynolds number. Primes denote differentiation with respect to the dimensionless variable y. The length scale is the displacement thickness $\hat{\delta}$,

$$\hat{\delta} = \int_0^\infty (1 - \overline{U})\, d\hat{y},$$

and the velocity scale is the edge velocity $\widehat{U}(\hat{x})$. The non-dimensional mean velocity $\overline{U}$ is determined by the boundary-layer equation in terms of the pressure distribution. For the flow over an aerofoil, $\overline{U}$ is generally expressed as a function of the non-dimensional coordinate η_b,

$$\eta_b = \hat{y}\left(\frac{\widehat{U}_\infty}{\hat{\nu}\hat{x}}\right)^{1/2}, \qquad (2.2)$$

where $\widehat{U}_\infty$ is the free stream velocity, $\hat{\nu}$ is the kinematic viscosity and the subscript b denotes the boundary layer flow.

The homogeneous equation (2.1) with vanishing velocity components on the wall and at infinity defines an eigenvalue problem for the parameters α, ω and R. For boundary layer flows it is not straightforward to calculate eigenvalues because serious numerical difficulties arise at large Reynolds number because the equation is stiff. Because of this, a number of numerical methods have been developed to numerically integrate the Orr-Sommerfeld equation (for details, see Drazin & Reid 1981). One such scheme is the compound matrix method developed by Davey (1982), which is known to be very reliable, but time-consuming. If it is necessary to calculate eigenvalues of the boundary layer on a wing at a number of streamwise locations at various design conditions the computational effort is considerable. However, it turns out that velocity profiles on these wings are very close to those of the Falkner-Skan family over two-dimensional wedges. The mean velocity, $\overline{U}(\eta_f) = f'(\eta_f)$, is determined by the boundary-layer equation

$$f''' + ff'' + \beta(1 - f'^2) = 0,$$

where β is the pressure gradient parameter, the non-dimensional coordinate η_f and the streamfunction $f(\eta_f)$ are defined by

$$\eta_f = \hat{y}\left(\frac{\widehat{U}(\hat{x})}{(2-\beta)\hat{\nu}\hat{x}}\right)^{1/2}, \qquad (2.3)$$

and

$$f(\eta_f) = \frac{\widehat{\psi}(\hat{x}, \hat{y})}{((2-\beta)\widehat{U}(\hat{x})\hat{\nu}\hat{x})^{1/2}},$$

the subscript f denotes the Falkner-Skan flow. The pressure gradient is the single parameter that determines the shape of Falkner-Skan profiles. Thus β is the key factor in approximating the boundary layer profiles with the Falkner-Skan family profiles. However, to match the boundary layer profiles with the Falkner-Skan family there is a second parameter to be determined apart from β, because the streamwise coordinate $\hat{x}$ on the wing is not the same quantity as that along the wedge flow. Thus $\hat{x}$'s have different meanings in the definitions of η_b and η_f of (2.2) and (2.3) though $\hat{y}$ is the same. There is a second factor, say $\gamma(\hat{x})$, that links these two variables. Suppose

$$\eta_f = \frac{\hat{y}}{\kappa(\hat{x})} \quad \text{and} \quad \eta_b = \frac{\hat{y}}{\kappa(\hat{x})}\gamma(\hat{x}),$$

where κ is a common factor and $\hat{x}$ is the same quantity now, we have

$$\eta_b = \gamma(\hat{x})\eta_f.$$

Consequently for the displacement thickness $\hat{\delta}$ and momentum thickness $\hat{\theta}$ we have

$$\hat{\delta}_f = \kappa(\hat{x}) \cdot \delta_f, \qquad \hat{\delta}_b = \kappa(\hat{x}) \cdot \delta_b/\gamma(\hat{x}), \tag{2.4}$$

and

$$\hat{\theta}_f = \kappa(\hat{x}) \cdot \theta_f, \qquad \hat{\theta}_b = \kappa(\hat{x}) \cdot \theta_b/\gamma(\hat{x}), \tag{2.5}$$

where δ and θ denote non-dimensional quantities. For the Falkner-Skan family, both δ_f and θ_f are functions of β,

$$\delta_f = \eta_{f\infty} - f(\eta_{f\infty}),$$

and

$$\theta_f = \frac{f''(0) - \beta\delta_f}{1+\beta}.$$

There are different ways of determining the two parameters β and γ from the given boundary layer data. Since the displacement thickness has been used as the length scale in deriving the non-dimensional Orr-Sommerfeld equation, we have to keep it constant for the two profiles and obtain the second equation by matching another physical quantity. One way of doing this is by matching the momentum thicknesses, *i.e.*

$$\hat{\delta}_f = \hat{\delta}_b \qquad \text{and} \qquad \hat{\theta}_f = \hat{\theta}_b. \tag{2.6}$$

In terms of (2.4) and (2.5), this leads to

$$\frac{\delta_b}{\theta_b} = \frac{\delta_f}{\theta_f}, \tag{2.7}$$

which is the relation that has to be satisfied to find the corresponding value of $\beta(\hat{x})$ for the boundary layer profile. This can be done by iteration.

The second way of matching is to require the second derivatives of the two profiles to be the same on the wall, *i.e.*

$$\hat{\delta}_f = \hat{\delta}_b \qquad \text{and} \qquad \frac{d^2\overline{U}_f}{d\eta_f^2}(0) = \frac{d^2\overline{U}_b}{d\eta_f^2}(0). \tag{2.8}$$

Since

$$\frac{d^2\overline{U}_f}{d\eta_f^2}(0) = -\beta$$

and

$$\frac{d^2\overline{U}_b}{d\eta_f^2}(0) = \gamma^2\frac{d^2\overline{U}_b}{d\eta_b^2}(0),$$

we have

$$\delta_b^2\frac{d^2\overline{U}_b}{d\eta_b^2}(0) = -\beta\delta_f^2 \tag{2.9}$$

to determine the value of β, which again can be found by iteration. In neither case does γ appear in the final calculation.

Thus the estimation of eigenvalues of the boundary layer can be reduced to that of calculating eigenvalues of the Falkner-Skan family. It would be possible to pre-calculate massive numbers of eigenvalues for the Falkner-Skan family with different values of β to create a vast look-up table, but this is not the best approach.

3. Padé approximants

Here an approximate description of the dispersion of the eigenvalues is used. Three methods have been used in the past. They are based on the fact that the Orr-Sommerfeld equation defines the complex eigenvalue ω as an analytic function of the complex wavenumber α and Reynolds number R except at some isolated points and can therefore be expressed by an elementary analytic function, such as a power series (Gaster & Jordinson 1975) or a rational-fraction function of α and R. It has been shown by Jiang (1990) that the Padé approximant method (Baker & Graves-Morris 1981) provides a better solution than the power series coupled with the Shanks nonlinear transformation (Gaster 1978). A two-variable Padé approximant is used to represent the eigenvalue relation for the Falkner-Skan velocity profile with a given β.

A two-variable Padé approximant defined by Chisholm (1973) can be obtained from a two-variable power series. Thus a two-variable power series for the eigenfrequency ω is formed as a function of both the complex wavenumber α and Reynolds number R.

It is important to treat the Reynolds number as a complex variable. Firstly, it enables the eigenvalues to be expanded in a complex Reynolds number plane so that their properties can be examined more efficiently. Secondly, Squire's transformation can then be used to reduce the three-dimensional eigenvalue problem appropriate to oblique waves to that of a two-dimensional one. This is because for complex wavenumbers, Squire's transformation defines a complex Reynolds number for the two-dimensional problem even if it is real in the three-dimensional case. Therefore, it is sufficient to discuss the two-dimensional dispersion relation $\Delta(\alpha, \omega, R) = 0$.

To construct a power series for the function $\omega(\alpha, R)$ from the original differential equation (2.1), $\omega(\alpha, R)$ is expressed as a Taylor series of the form

$$A_{mn}(\alpha - \alpha_0)^m (R - R_0)^n,$$

where α_0 and R_0 are the centres of the expansion inside the analytic regions of the complex α-plane and R-plane. The coefficients can be determined by the derivatives of $\omega(\alpha, R)$ at the center. The values of the derivatives can be calculated by the Cauchy integral theorem in terms of values of the function along closed contours in the independent variable planes. It is convenient to choose circular contours within the analytic region of $\omega(\alpha, R)$, thus

$$A_{mn} = \frac{1}{4\pi^2 r_\alpha^m r_R^n} \int_0^{2\pi} \int_0^{2\pi} \omega(\alpha, R) \, e^{-im\theta_\alpha} e^{-in\theta_R} d\theta_\alpha d\theta_R,$$

where r_α and r_R are respectively the radii of the circular regions. Since r_α and r_R are usually less than unity, it is wise to avoid dividing r_α^m and r_R^n in the numerical calculation by defining

$$\omega(\alpha, R) = \sum_{n=0}^{N-1} \sum_{m=0}^{M-1} B_{mn} \left(\frac{\alpha - \alpha_0}{r_\alpha}\right)^m \left(\frac{R - R_0}{r_R}\right)^n. \qquad (3.1)$$

By discretising the circles into K and L points, B_{mn} is calculated numerically by the double summation

$$B_{mn} = \frac{1}{KL} \sum_{l=0}^{L-1} \sum_{k=0}^{K-1} \omega_{kl} \exp(-i2\pi mk/K) \exp(-i2\pi nl/L), \qquad (3.2)$$

where the values of ω_{kl} are found from the Orr-Sommerfeld equation on the circle $\alpha_k = \alpha_0 + r_\alpha e^{i\theta_k}$ and $R_l = R_0 + r_R e^{i\theta_l}$.

In this way, $|B_{mn}|$ is generally a monotonically decreasing function of the summation index m and n. The decreasing rate can be examined by the contour plot of $\log|B_{mn}|$ in the (m, n)-plane. The contours will be a set of almost parallel lines with constant $m+n$. The contour level decreases as $m+n$ increases, which indicates that ω can be approximately represented by (3.1). However, as ω is a function of two independent variables, there are different ways of constructing power series, such as $\omega(\alpha^2, R)$, $\omega(\alpha^2, \alpha R)$ and so on. Our trial studies showed that the expansion for $\omega(\alpha^2, R)$ was more convergent than that for $\omega(\alpha, R)$, and for $\omega(\alpha^2, \alpha R)$ was even better, in terms of the smoothness of $\log|B_{mn}|$ as a function of m and n. For the expansion with α^2 and αR as independent variables, the contour plot of $\log|B_{mn}|$ showed that the values of $\log|B_{mn}|$ generally decreased linearly as $m + n$ increased but the slope had a sudden change for small n where $\log|B_{m2}| << \log|B_{m1}|$. This means that $|\partial\omega/\partial(\alpha R)|$ is much smaller than $|\omega|$ at the expansion point $(\alpha R)_0$ for given α. When a power series for the wavespeed $c = \omega/\alpha$ was constructed by the same procedure with its coefficients denoted by D_{mn}, we found that its coefficient contours were much smoother. In addition, for large values of m and n, $|D_{mn}|$ is smaller than $|B_{mn}|$, implying that the series for c is more accurate than that for ω for the same number of terms. It may be noticed that the above results are actually determined by the structure of the Orr-Sommerfeld equation (2.1) itself, where α^2, αR and ω/α are three natural parameters of the equation. Thus we will use the double power series

$$c(\alpha^2, \alpha R) = \frac{\omega}{\alpha} = \sum_{n=0}^{N-1} \sum_{m=0}^{M-1} D_{mn} \left(\frac{\alpha^2 - \alpha_0^2}{r_{\alpha^2}}\right)^m \left(\frac{\alpha R - (\alpha R)_0}{r_{\alpha R}}\right)^n, \qquad (3.3)$$

where r_{α^2} and $r_{\alpha R}$ are respectively the radii of the expansion circles in the complex α^2 and αR planes. The coefficients D_{mn} were obtained in a similar way to B_{mn} in (3.2) with eigenvalues calculated on the circle $(\alpha R)_l = (\alpha R)_0 + r_{\alpha R} e^{i\theta_l}$ for every α taken from $\alpha_k^2 = \alpha_0^2 + r_{\alpha^2} e^{i\theta_k}$.

The two-variable diagonal Padé approximants of Chisholm are defined to have a given maximum power in each variable, rather than to have a given total maximum power. The $[L/L]$ Padé approximant is thus of the form

$$[L/L](\lambda_{\alpha^2}, \lambda_{\alpha R}) = \sum_{\mu=0}^{L} \sum_{\nu=0}^{L} p_{\mu\nu} \lambda_{\alpha^2}^{\mu} \lambda_{\alpha R}^{\nu} \Big/$$

$$\sum_{\mu=0}^{L}\sum_{\nu=0}^{L} q_{\mu\nu}\lambda_{\alpha^2}^{\mu}\lambda_{\alpha R}^{\nu}, \tag{3.4}$$

where λ_{α^2} and $\lambda_{\alpha R}$ denote $(\alpha^2-\alpha_0^2)/r_{\alpha^2}$ and $(\alpha R-(\alpha R)_0)/r_{\alpha R}$ respectively. The coefficients $p_{\mu\nu}$ and $q_{\mu\nu}$ are determined by the coefficients D_{mn} of the series (3.3). Without loss of generality, (3.4) can be normalized by taking $q_{00}=1$. The number of coefficients to be determined is then

$$(L+1)^2+\left[(L+1)^2-1\right]=2L^2+4L+1.$$

For example, if $L=5$, the above result means that there are 71 coefficients to be determined.

In general, the coefficients in the $[L/L]$ Padé approximant can be determined by formally letting

$$\left[\sum_{\mu=0}^{L}\sum_{\nu=0}^{L} q_{\mu\nu}\lambda_{\alpha^2}^{\mu}\lambda_{\alpha R}^{\nu}\right]\left[\sum_{n=0}^{\infty}\sum_{m=0}^{\infty} D_{mn}\lambda_{\alpha^2}^{m}\lambda_{\alpha R}^{n}\right]$$

$$=\sum_{\mu=0}^{L}\sum_{\nu=0}^{L} p_{\mu\nu}\lambda_{\alpha^2}^{\mu}\lambda_{\alpha R}^{\nu}+o(\lambda_{\alpha^2}^{k}\lambda_{\alpha R}^{2L-k}).$$

The second term on the right hand side indicates that coefficients of all terms of total order less than $2L+1$ are equated. The number of equations is

$$\sum_{k=1}^{2L+1} k=2L^2+3L+1.$$

Since

$$p_{\mu\nu}=q_{\mu\nu}=0 \quad \text{for} \quad \mu>L \ \text{ or } \ \nu>L,$$

we have $(L+1)^2$ equations from

$$\sum_{\sigma=0}^{\mu}\sum_{\tau=0}^{\nu} q_{\sigma\tau}D_{\mu-\sigma,\nu-\tau}=p_{\mu\nu} \tag{3.5}$$

$$\text{for} \quad 0\le\mu<L,\ 0\le\nu\le L,$$

and $L(L+1)$ equations from

$$\sum_{\sigma=0}^{L}\sum_{\tau=0}^{\nu} q_{\sigma\tau}D_{\mu-\sigma,\nu-\tau}=0 \tag{3.6}$$

$$\text{for} \quad 0\le\nu<L,\ L<\mu\le 2L-\nu,$$

$$\sum_{\sigma=0}^{\mu}\sum_{\tau=0}^{L} q_{\sigma\tau}D_{\mu-\sigma,\nu-\tau}=0 \tag{3.7}$$

$$\text{for} \quad 0\le\mu<L,\ L<\nu\le 2L-\mu.$$

In addition L equations are provided by equating the sums of coefficients of the L pairs of terms

$$\lambda_{\alpha^2}^{k}\lambda_{\alpha R}^{2L+1-k} \quad \text{and} \quad \lambda_{\alpha^2}^{2L+1-k}\lambda_{\alpha R}^{k} \quad (k=1,2,\cdots,L),$$

that is,

$$\sum_{\sigma=0}^{k}\sum_{\tau=0}^{L}(q_{\sigma\tau}D_{k-\sigma,2L+1-k-\tau}$$

$$+q_{\tau\sigma}D_{2L+1-k-\tau,k-\sigma})=0 \quad (1\le k\le L). \tag{3.8}$$

Thus the $(L+1)^2-1$ values of $q_{\mu\nu}$ are found from (3.6) to (3.8). The additional $(L+1)^2$ values of $p_{\mu\nu}$ are then given by the summation in (3.5). For different $[L/L]$ diagonal Padé approximants, the zeros and poles in the complex α-plane for fixed R and in the complex R-plane for fixed α can be found. The real zeros or poles, if any, of the function $\omega(\alpha,R)$ will appear consistently in this sequence. An optimum approximant can then be chosen such that it is free from all the artificial poles and zeros in the region to be studied, leaving only those which are inherent to the physical problem.

The convergence region of a two-variable Padé approximant is difficult to visualize since it is four-dimensional. Figure 3.1 shows the error contours of $\log|\omega_{PA}-\omega_{OS}|$ in the real (α,R)-plane for the case of Blasius flow, where ω_{PA} are obtained with different orders of Padé approximants obtained from a power series with $\alpha_0^2=0.06$, $r_{\alpha^2}=0.03$, $(\alpha R)_0=550$, $r_{\alpha R}=250$, $K=32$, $L=48$ and ω_{OS} are calculated directly from the Orr-Sommerfeld equation. Agreement between the Padé estimate and that provided by the solution of the Orr-Sommerfeld equation was very good close to the centres of expansion. The [5/5] Padé approximant gives 6 decimal accuracy within the stability loop. The CPU time for calculating the same 60×60 eigenvalues from this approximant is 9.1 seconds, some 2500 times faster than by direct eigenvalue evaluation.

The Padé approximant turns out to be less accurate for small values of α and R. This difficulty with small α arises because of the inherent singular property of the eigenfrequency ω for the very long waves. This singular point is bound to affect not only the Padé approximant method, but also other analytic representations of $\omega(\alpha,R)$. On the other hand, the solutions of the Orr-Sommerfeld equation at low Reynolds numbers should only be accepted with reservation since the fundamental assumption that the undisturbed flow can be approximated by the parallel flow model of the boundary-layer equation becomes unrealistic. The failure of the Padé approximant method at small R may well produce errors no greater than those arising from using the parallel flow approximation at low Reynolds numbers. In the transition-prediction calculation for air-

craft wings, the calculation of eigenvalues for small values of αR are not required.

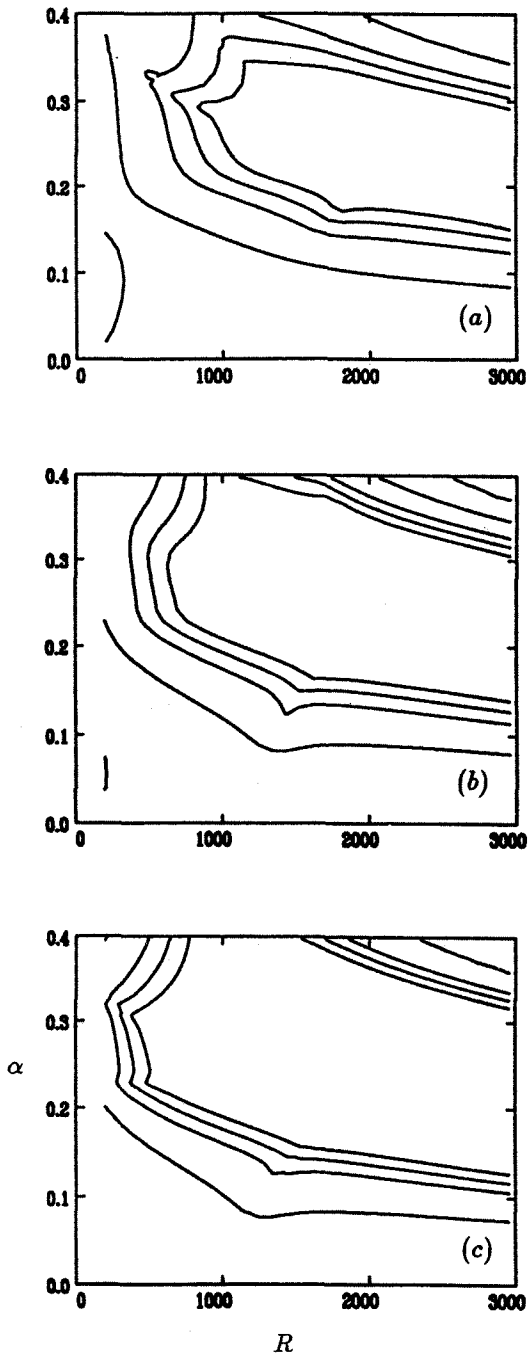

Figure 3.1 Contours of $\log|\omega_{PA} - \omega_{OS}|$ where ω_{PA} are calculated from the Padé approximant (3.4) with orders of $(a)L = 5$, $(b)L = 7$, $(c)L = 9$ and ω_{OS} from the Orr-Sommerfeld equation. Contour levels are -8, -7, -6, -4, -2.

4. Amplification curves

In the previous two sections the two basic steps of the rapid scheme for estimating eigenvalues and then the amplitude ratio have been outlined. The given boundary layer velocity profiles are fitted to the Falkner-Skan family so as to obtain the corresponding pressure gradient parameter β and using Padé approximants to represent the eigenvalue relation for the Falkner-Skan profile.

The representation of the eigenvalue relation for a general Falkner-Skan profile can be achieved by considering a set of Padé approximants covering a range of β's. Then by suitable interpolation the Padé coefficients can be determined for any specified pressure gradient parameter. The total 24 two-variable power series for a number of values of β were formed. The increment chosen for the values of β was not constant since the eigenfrequency for the given α and R changes more rapidly for the smaller value of β than for larger value of β.

β	$(\alpha R)_0$	α_0^2	r_{α^2}
0.00	550	0.060	0.0300
0.02	570	0.057	0.0270
0.04	590	0.055	0.0260
0.06	610	0.053	0.0250
0.12	670	0.048	0.0230
0.20	750	0.042	0.0210
0.30	850	0.040	0.0200
0.45	1000	0.037	0.0185
0.60	1150	0.034	0.0170
0.80	1350	0.030	0.0150
1.00	1550	0.026	0.0130

Table 1. Numerical values of the expansion point and radius for some of the power series set. The same $r_{\alpha R}$, 250, is used for all the series.

In constructing Padé approximants from the double power series only the coefficients of terms whose total power are less than $2L+1$ were used. That is to say, the coefficients $p_{\mu\nu}$ and $q_{\mu\nu}$ in the Padé approximant were determined by the coefficients D_{mn} on the bottom left corner in the (m,n)-plane. Naturally, it is thought that a better Padé approximant is formed when the contours of $\log|D_{mn}|$ in the (m,n)-plane are roughly aligned with the $m+n = constant$ lines. This can be achieved by selecting appropriate expansion points and radii in constructing the power series

for different values of β. Here $r_{\alpha R}$ has been kept constant at a value of 250, together with smaller values of α_0^2, r_{α^2} and larger $(\alpha R)_0$ as β increased. Some of the numerical values were given in Table 1. Two of the contour plots of $\log|D_{mn}|$ in the (m,n)-plane are shown in figure 4.1 for $\beta = 0.06$ and 0.45, respectively, indicating the general behaviour of the coefficients.

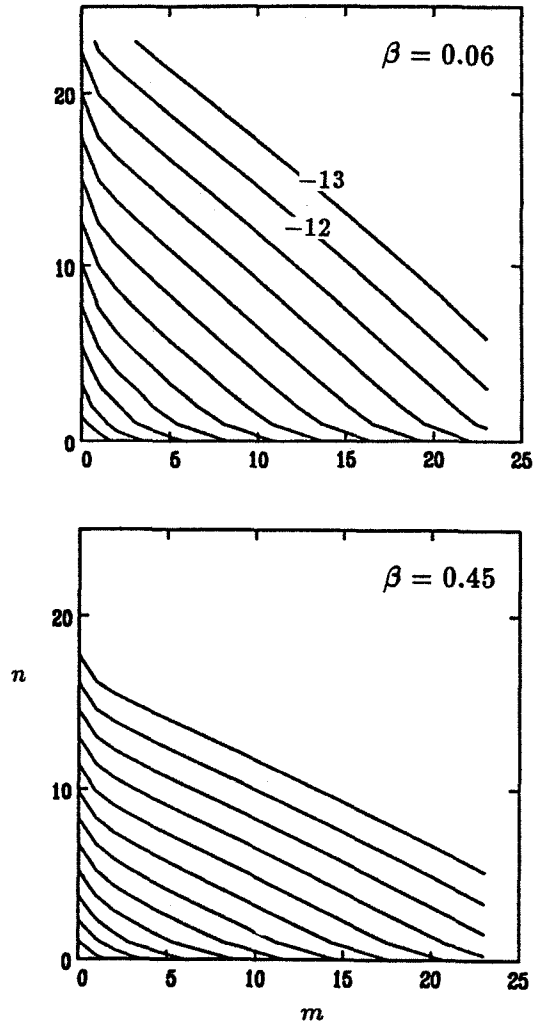

Figure 4.1 Diagram of the contour plots of $\log|D_{mn}|$ for $\beta = 0.06$ and 0.45. The contour levels are $-2, -3, -4, -5, -6, -7, -8, -9, -10, -11, -12, -13$.

From this set of power series, the corresponding Padé approximants were constructed. It was found that the order of [5/5] Padé approximant generally gave accurate eigenvalues within the stability loop. The curves of constant temporal amplification rates found by [5/5] approximants for $\beta = 0.06$ and 0.45 are shown in figure 4.2. These plots can be compared with those given by Obremski, Morkovin & Landahl (1969), showing only minor differences. For an arbitrary value of β, eigenvalues were calculated from the interpolated Padé formed from the four neighbouring values of β.

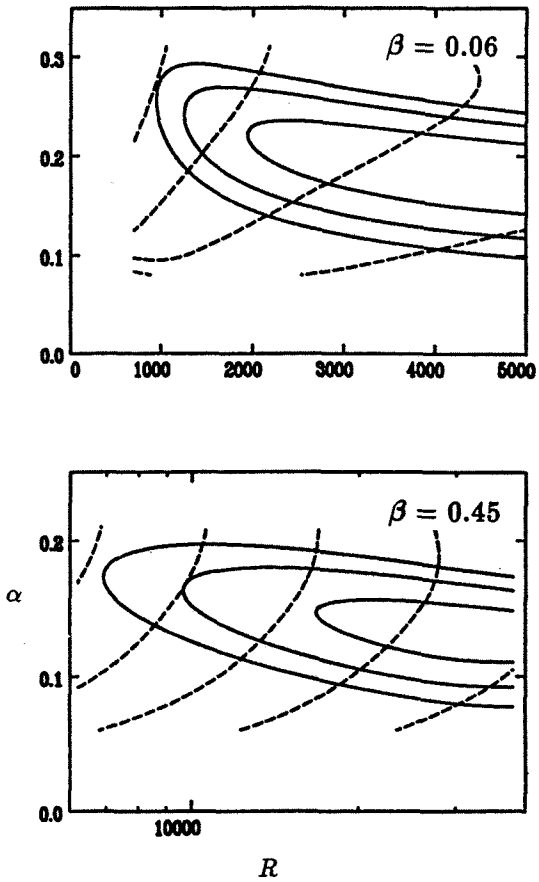

Figure 4.2 Stability diagram of the Falkner-Skan flow for $\beta = 0.06$ and 0.45. The solid curves are for the constant temporal amplification rates $\omega_i \times 100$ and dashed ones for the constant wavespeed c_r.

For the transition-prediction study the quantity of primary interest is the integral of the spatial amplification rate at a constant frequency. It was necessary to find the wavenumber α for given (ω, R). This can be done by constructing a set of Padé approximants for α as a function of (ω, R) or by using $\omega(\alpha^2, \alpha R)/\alpha$ through an iteration to find the spatial mode. It turned out that better results were obtained by using the approximant for $\omega(\alpha^2, \alpha R)/\alpha$ to calculate the

spatial amplification rate by iteration.

A test case was used to illustrate the detailed procedure involved in calculating the wave growth in laminar boundary layers on aircraft wings. The flow conditions together with the mean velocity and its second derivative distribution on a coarse grid were supplied by the Research Department of British Aerospace at Hatfield. The Mach number was 0.1, chord length 4 meters and Reynolds number based on the chord length was 10×10^6. The distribution of the pressure coefficient C_p and non-dimensional edge velocity U are shown in figure 4.3.

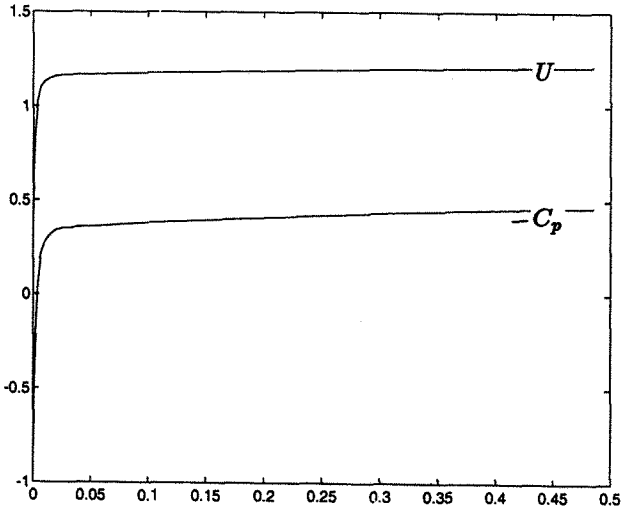

Figure 4.3 Distributions of the non-dimensional edge velocity U and pressure coefficient C_p along the chord length for the test case.

The data file contained values of η_j, $\overline{U}(\eta_j)$ and $\overline{U}''(\eta_j)$ at about 400 positions of η for approximately 40 streamwise locations up to $\hat{x}/C \approx 0.5$, where $\hat{x}$ is the streamwise distance from the leading edge and C is the chord length. The step size $\Delta\eta$ was not constant, being smaller near the wall than near the outer boundary. In order to check the accuracy of the scheme it was also necessary to calculate eigenvalues for these non-similar boundary layers by solving the Orr-Sommerfeld equation directly. This required the mean velocity distribution with a finer step size $\Delta\eta$. The profile data supplied was used in conjunction with a cubic spline interpolation scheme to provide the fine steps needed for the direct Orr-Sommerfeld equation solution. This had to be carried out at each streamwise location. The displacement thickness δ_b and momentum thickness θ_b were obtained by the numerical summation of $\overline{U}(\eta)$. Since $\overline{U}''$ in (2.1) is the second derivative of the mean velocity with respect to the dimensionless variable y, $y = \hat{y}/\hat{\delta}_b$,

$$\hat{y} = \eta_b \left(\hat{\nu}\hat{x}/\widehat{U}_\infty\right)^{1/2} \quad \text{and} \quad \hat{\delta}_b = \delta_b \left(\hat{\nu}\hat{x}/\widehat{U}_\infty\right)^{1/2},$$

we have

$$y = \frac{\eta_b}{\delta_b} \quad \text{so that} \quad \frac{d^2\overline{U}_b}{dy^2} = \delta_b^2 \frac{d^2\overline{U}_b}{d\eta_b^2}.$$

Once the value of β had been obtained at every streamwise location $\hat{x}$ for a laminar boundary layer it was a fairly straightforward matter to compute growth rates. With the displacement thickness $\hat{\delta}_b(\hat{x})$ and the edge velocity $\widehat{U}(\hat{x})$ being the length scale and the velocity scale respectively, the Reynolds number $R(\hat{x})$ is given by

$$R = \frac{\widehat{U}\hat{\delta}_b}{\hat{\nu}}. \tag{4.1}$$

For a disturbance of constant dimensional frequency $\hat{\omega}$, the non-dimensional frequency $\omega(\hat{x})$ is given by

$$\omega = \frac{\hat{\omega}\hat{\delta}_b}{\widehat{U}}.$$

Instead of showing results for the constant $\hat{\omega}$, it is convenient to use a non-dimensional frequency F,

$$F = \hat{\omega}\hat{\nu} \Big/ \widehat{U}_\infty^2.$$

In this case,

$$\omega = F \left(\widehat{U}_\infty \Big/ \widehat{U}\right)^2 R. \tag{4.2}$$

The amplitude ratio is determined by

$$\ln\left(\frac{A}{A_0}\right) = -\int_{\hat{x}_0}^{\hat{x}} \frac{\alpha_i}{\hat{\delta}_b} d\hat{x}, \tag{4.3}$$

where α_i is the imaginary part of the wavenumber $\alpha(\omega, R) = \hat{\alpha}\hat{\delta}_b$, which is calculated by the Padé approximants through an iteration process. The lower integration limit $\hat{x}_0$ is the location where $\alpha_i = 0$. Some care was needed to find this point because there were only a limited number of profiles in the streamwise direction in that region. The value of α_i will jump from a positive value to a negative one from one location to the next. In the calculation, $\hat{x}_0$ is assumed to be given by

$$\hat{x}_0 = \hat{x}_- - \hat{\alpha}_{-i} \frac{\hat{x}_+ - \hat{x}_-}{\hat{\alpha}_{+i} - \hat{\alpha}_{-i}},$$

where $\hat{x}_-$ is the last location where $-\alpha_i(\hat{x}_-) < 0$ from the leading edge and $\hat{x}_+$ is the first location where $-\alpha_i(\hat{x}_+) > 0$. The contribution from $\hat{x}_0$ to $\hat{x}_+$ for the integral (4.3) is given by

$$-\int_{\hat{x}_0}^{\hat{x}_+} \hat{\alpha}_i d\hat{x} = -\frac{\hat{x}_+ - \hat{x}_-}{2} \frac{\hat{\alpha}_{+i}^2}{\hat{\alpha}_{+i} - \hat{\alpha}_{-i}},$$

which is really very small.

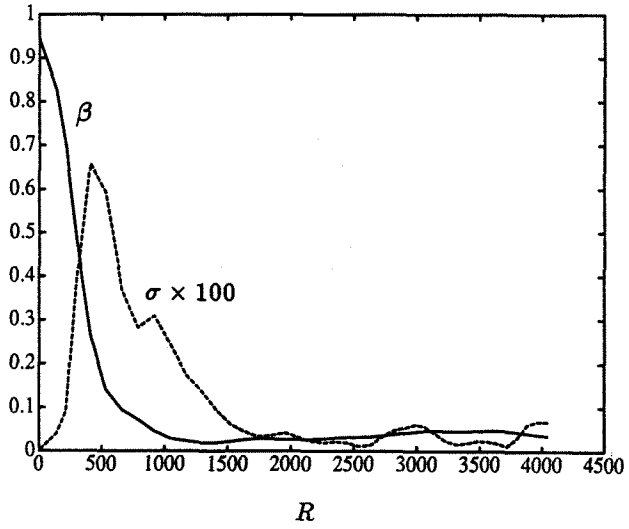

Figure 4.4 Distributions of the pressure gradient parameter β and the standard deviations σ, obtained by matching $\hat{\delta}$ and $\hat{\theta}$.

The standard deviation

$$\sigma = \left\{ \frac{1}{M} \sum (\overline{U}_b - \overline{U}_f)^2 \right.$$

$$\left. + \frac{1}{M} \sum \left[\frac{d^2\overline{U}_b}{d\eta_b^2} - \left(\frac{\delta_f}{\delta_b}\right)^2 \frac{d^2\overline{U}_f}{d\eta_f^2} \right]^2 \right\}^{1/2},$$

where the factor δ_f/δ_b in front of $d^2\overline{U}_f/d\eta_f^2$ is due to the requirement of $\hat{\delta}_f = \hat{\delta}_b$, is a quantity used to examine how close the BAe profiles were approximated by those of Falkner-Skan. The matched values of β, together with the standard deviations $\sigma \times 100$, obtained by matching $\hat{\delta}$ and $\hat{\theta}$ are presented in figure 4.4. To show the results more conveniently β has been plotted against the Reynolds number R whose dependence on the streamwise location $\hat{x}$ is determined by (4.1). As can be seen, this aerofoil has a relatively flat pressure distribution over much of the surface and only small variations in β are evident covering the range 0.0 to 0.1 in the zone where the Reynolds number is large enough to allow amplification. The value of the standard deviation is greatest at the location where $-C_p$ stops increasing rapidly and begins a slow increase. When both the BAe profiles and Falkner-Skan profiles are plotted around these locations large values of σ arise mainly from the discrepancy between the second derivative distributions. However, since the Reynolds number is small near the leading edge these first few locations do not contribute to the integral (4.3). The total amplification curves for various frequencies for this test case are presented in figure 4.5, where the curves refer to the direct Orr-Sommerfeld solutions and the symbols refer to estimates provided by the Padé approximant method with the values of β determined by matching $\hat{\delta}$ and $\overline{U}''(0)$. The error for the value of N-factor is less than 3%.

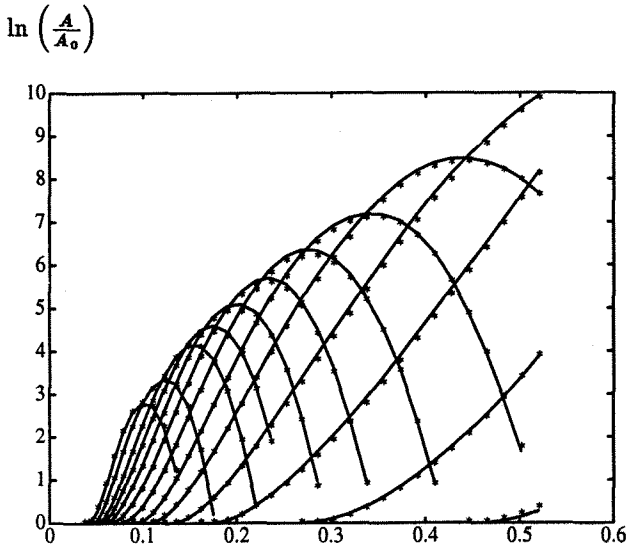

Figure 4.5 Total amplification curves for various frequencies, where the curves are obtained by solving the Orr-Sommerfeld equation and the symbols by using the Padé approximant method.

5. Discussion

From the result of the test case it appears that the numerical scheme developed in this paper is sufficiently accurate for the purpose of estimating transition by the amplification ratio. The method can speed up the calculation of the amplification ratio by a large factor without significant loss of accuracy. The re-

sult obtained by matching the momentum thickness is similar to that obtained by matching the second derivative at the wall. It is therefore only necessary to provide values of the displacement thickness distribution and the second derivative on the wall to do the fitting for a particular wing design. Alternatively, if there is a difficulty in providing accurate second derivatives, profile matching can also be used to achieve reliable result.

It turned out that most of the Padé approximants that have been constructed will not be used in the practical calculation since $-\alpha_i < 0$ when $R < 500$. This suggests that it might be worth constructing more Padé approximants in the range $-0.1 \leq \beta \leq 0.1$.

Acknowledgment

This work was supported by the Research Department of British Aerospace at Hatfield.

Reference

Baker, G. A., Jr & Graves-Morris, P. R., 1981 *Padé Approximants.* In: Encyclopaedia of mathematics and its applications. Addison-Wesley Publishing Company.

Chisholm, J. S. R. 1973 Rational approximants defined from double power series, *Math. Comp.*, **27**, 841-848.

Davey, A.,1982 A difficult numerical calculation concerning the stability of the Blasius boundary layer, In *Stability in the Mechanics of Continua*, (ed: F.H. Schroeder), 365-372.

Drazin, P. G. & Reid, W. H. 1981 *Hydrodynamic Stability.* Cambridge University Press.

Gaster, M. 1968 The development of three dimensional wave packets in a boundary layer. *J. Fluid Mech.*, **32**, 173-184.

Gaster, M. 1978 Series representation of the eigenvalues of the Orr-Sommerfeld equation. *J. Comp. Phys.*, **29**(2), 147-162.

Gaster, M. & Jordinson, R. 1975 On the eigenvalues of the Orr-Sommerfeld equation. *J. Fluid Mech.*, **72**(1), 121-133.

Jiang, F. 1990 The development of linear wave packets in unbounded shear flows. Ph.D thesis. Cambridge University Engineering Department.

Mack, L. M. 1977 Transition and laminar instability. *JPL publication 77-15.*

Obremski, H. J., Morkovin, M. V. & Landahl, M. T. 1969 A portfolio of stability characteristics of incompressible boundary layers. AGARDograph 134, North Atlantic Treaty Organization, Neuilly Sur Seine, France.

Shanks, D. 1955 Nonlinear transformations of divergent and slowly convergent sequences. *J. Math. & Phys.*, **34**, 1-42.